

Cosmological model with Gong-Zong Parametrization in $f(R, L_m)$ gravity

Romanshu Garg^{1*}, Tanmoy Chowdhury^{2†}, G. P. Singh^{1‡}, Farook Rahaman^{2§}

¹ Department of Mathematics,
Visvesvaraya National Institute of Technology, Nagpur, 440010, Maharashtra India.

² Departments of Mathematics,
Jadavpur University, Kolkata 700032, West Bengal, India.

Abstract

In this study, we investigate the cosmic expansion scenario by using the Gong - Zhang parameter in the framework of $f(R, L_m)$ gravity, for a specific form of $f(R, L_m) = \frac{R}{2} + L_m^n$. We get the Hubble parameters in terms of the red-shift (z) obtained using the Gong-Zhang parameter $\omega = \frac{w_0}{z+1}$. Using Bayesian statistical methods based on the χ^2 -minimization technique, we obtain the median values of this model's model parameters for the cosmic chronometer and Joint (CC+Pantheon) data sets. We deliberate about the behaviour of key cosmological parameters, for instance, the deceleration parameter, and equation of state, energy density (ρ), pressure (p), and the effect of the energy conditions with median values of the model parameters. Additionally, we have examined the behavior of the Statefinder diagnostics and determine the universe's current age of this model.

Keywords: $f(R, L_m)$ gravity, Statefinder diagnostics, Equation of state parameter, Energy conditions, Universe's age.

1 Introduction

Astronomical studies [1–3] have confirmed the expanding rate of the cosmos, which is an intriguing discovery of the observable universe. Afterwards, theoretical cosmologists became interested in creating cosmological models that depicted an accelerated phase of the universe's expansion. Multiple theoretical cosmologists have put forward models that either modify Einstein's field equations or suggest other theories of gravity in response to the universe's acceleration. A more appropriate cosmological models to explain the current growth in the universe's expansion has been proposed, based on the several types of dark energy that produce negative pressure. It is generally agreed that the dynamical cosmological term Λ is one of the most promising dark energy candidates [4, 5]. However, there are multiple difficulties with the Λ term model, including coincidence issues and fine tuning. To deal with these present cosmological problems, various approaches have been proposed in the last few decades. Nowadays, the modified theory of gravity technique is the most often used option for resolving

*romanshugarg18@gmail.com

†tanmoych.ju@gmail.com

‡gpsingh@mth.vnit.ac.in

§rahaman@associates.iucaa.in

current cosmological issues. One of the most well-known ideas to the dark content problem of the universe is the $f(R)$ gravity [6, 7] which is a modification of General Relativity. With the evolving time, several other modified theories are also widely explored[8–16].

Further cooperation the framework, a relation in between the Ricci scalar R with L_m as matter Lagrangian density was sorted, which tends to the gravitational development $f(R, L_m)$. Harko and Lobo [17] show that this theory probes more general relations between matter and geometry. Still, this approach violates the equivalence principle, It was also mentioned that solar system observations impose stringent restrictions on such infractions [18–21]. Among the most complete gravitational theories represented on Riemannian space [22–24] is the $f(R, L_m)$ framework, which offers novel perspectives on the intricate relationships between the geometries of cosmology-astrophysics and matter. Due to the presence of matter, Mathematical formation i.e. field equations of $f(R, L_m)$ gravity, and the $f(R)$ model, differ from each other and GR, but they are equal in empty space of time [17, 25]. In connection with the $f(R, L_m)$ gravity, numerous further studies have been finished[26–31].

The following work is divided into seven sections, detailed written as: In Sec. (2), we discuss an overview of the $f(R, L_m)$ gravity theory. Sec. (3) introduced the field equations within the FLRW metric context. In Sec. (4), we discuss the Hubble parameter of the models in terms of red-shift for specific form of the $f(R, L_m)$ cosmological model. Then next we introduced the Bayesian statistical methods in Sec. (5), we constrain the median values of free parameters via Cosmic Chronometer (CC) data and a combined data set (CC + Pantheon). In Sec. (6), we observe the graphical behaviour of the deceleration parameter for the parameters median values, together with a complete analysis of physical methods such as the EOS parameter (ω), pressure (p) and energy density (ρ), involve with their graphical illustrations. Furthermore, we examine the progress of all energy conditions and the statefinder diagnostic. We determine the age of the universe of this model. Finally, conclusions are given in the last section (7).

2 Overview of specified $f(R, L_m)$ gravity theory

In this section, we discuss a overview of modified gravity $f(R, L_m)$ and the action in $f(R, L_m)$ gravity takes the form [17].

$$S = \int f(R, L_m) \sqrt{-g} d^4x, \quad (1)$$

where, L_m defines as matter Lagrangian density and R refers to Ricci scalar .

We can define Ricci scalar (R) within the characteristics of Ricci tensor ($R_{\mu\nu}$) with metric tensor ($g^{\mu\nu}$), as given away below

$$R = g^{\mu\nu} R_{\mu\nu}, \quad (2)$$

where the $R_{\mu\nu}$ is inscribed in the resulting appearance as

$$R_{\mu\nu} = \partial_c \Gamma_{\mu\nu}^c - \partial_\mu \Gamma_{c\nu}^c + \Gamma_{\mu\nu}^c \Gamma_{dc}^d - \Gamma_{\nu d}^c \Gamma_{\mu c}^d, \quad (3)$$

where $\Gamma_{\beta\gamma}^\alpha$ signifies the mechanisms of Levi-Civita relation, defined as

$$\Gamma_{\beta\gamma}^\alpha = \frac{1}{2} g^{\alpha c} \left(\frac{\partial g_{\gamma c}}{\partial x^\beta} + \frac{\partial g_{c\beta}}{\partial x^\gamma} - \frac{\partial g_{\beta\gamma}}{\partial x^c} \right). \quad (4)$$

Using the action (1) with to the metric tensor $g_{\mu\nu}$, the field equation written as,

$$\frac{\partial f}{\partial R} R_{\mu\nu} + (g_{\mu\nu} \square - \nabla_\mu \nabla_\nu) \frac{\partial f}{\partial R} - \frac{1}{2} \left(f - \frac{\partial f}{\partial L_m} L_m \right) g_{\mu\nu} = \frac{1}{2} \left(\frac{\partial f}{\partial L_m} \right) T_{\mu\nu}, \quad (5)$$

where $T_{\mu\nu}$ is defined as the energy-momentum tensor for perfect fluid.

$$T_{\mu\nu} = \frac{-2}{\sqrt{-g}} \frac{\delta(\sqrt{-g}L_m)}{\delta g^{\mu\nu}}. \quad (6)$$

Using these field equations, we can construct a relationship between the Ricci scalar(R), the trace of the energy-momentum tensor T and the matter Lagrangian density (L_m).

$$R \left(\frac{\partial f}{\partial R} \right) + 2 \left(\frac{\partial f}{\partial L_m} L_m - f \right) + 3 \square \frac{\partial f}{\partial R} = \frac{1}{2} \left(\frac{\partial f}{\partial L_m} \right) T, \quad (7)$$

where the $\square I = \frac{1}{\sqrt{-g}} \partial_\mu (\sqrt{-g} g^{\mu\nu} \partial_\nu I)$ for any type of random function I.

To analyse the equations (5), we can substitute the covariant derivative with energy-momentum tensor, written as:

$$\nabla^\mu T_{\mu\nu} = 2 \nabla^\mu \log[f_{L_m}(R, L_m)] \frac{\partial L_m}{\partial g^{\mu\nu}}. \quad (8)$$

3 Motion equations in $f(R, L_m)$ gravity

To study the present cosmological model, we employ the flat Friedman–Lemaître–Robertson–Walker (FLRW) metric [32] definite as follows:

$$ds^2 = a^2(t) (dx^2 + dy^2 + dz^2) - dt^2, \quad (9)$$

where at a given time 't', the scale factor of cosmic expansion denotes as ' $a(t)$ '.

For the line element (9), the non-vanishing components of the Christoffel symbols are:

$$\Gamma_{pq}^0 = -\frac{1}{2} g^{00} \frac{\partial g_{pq}}{\partial x^0}, \quad \Gamma_{0q}^r = \Gamma_{q0}^r = \frac{1}{2} g^{r\lambda} \frac{\partial g_{q\lambda}}{\partial x^0}, \quad (10)$$

where the variables p, q and r defines as 1, 2 and 3.

By utilizing equation (3), the non-vanishing components of the Ricci tensor are written as:

$$R_0^0 = 3 \frac{\ddot{a}}{a}, \quad R_1^1 = R_2^2 = R_3^3 = \frac{\ddot{a}}{a} + 2 \left(\frac{\dot{a}}{a} \right)^2. \quad (11)$$

Thus, the Ricci scalar derived for the line elements (9) is,

$$R = 6 \left(\frac{\dot{a}}{a} \right)^2 + 6 \left(\frac{\ddot{a}}{a} \right) = 12H^2 + 6\dot{H}, \quad (12)$$

where $H = \frac{\dot{a}}{a}$ denotes as Hubble parameter.

For a perfect fluid, We characterise the stress energy-momentum tensor, that is specified by:

$$T_{\mu\nu} = (p + \rho) u_\mu u_\nu + p g_{\mu\nu}, \quad (13)$$

where p and ρ are defined as the isotropic pressure and the energy density of the cosmic fluid, and the components $u^\mu = (1, 0, 0, 0)$ are the components of the four velocities of the cosmic perfect fluid, defining that $u_\mu u^\mu = -1$.

The Friedmann equations that describe the dynamics relation of the universe in $f(R, L_m)$ gravity can be read as follows:

$$\frac{1}{2}(f - f_{L_m}L_m - f_R R) + 3H\dot{f}_R + 3H^2 f_R = \frac{1}{2}f_{L_m}\rho, \quad (14)$$

and

$$3H^2 f_R + \dot{H}f_R - \ddot{f}_R - 3H\dot{f}_R + \frac{1}{2}(-f + f_{L_m}L_m) = \frac{1}{2}f_{L_m}p. \quad (15)$$

4 Cosmological $f(R, L_m)$ model theory

We choose a specific form of $f(R, L_m)$ gravity [33] as follows:

$$f(R, L_m) = \frac{R}{2} + L_m^n, \quad (16)$$

where n is an arbitrary constant.

For this specified functional form of the $f(R, L_m)$ gravity model with $L_m = \rho$ [34], equation (14) and (15) become

$$3H^2 = (2n - 1)\rho^n, \quad (17)$$

and

$$2\dot{H} + 3H^2 = (n - 1)\rho^n - n\rho\rho^{n-1}. \quad (18)$$

The mathematical representation of the Equation of State (EOS) parameter is $\omega = \frac{p}{\rho}$. Then by using equations (17), (18) and $\dot{H} = -H(1+z)\frac{dH}{dz}$ we get the equation of state parameter ω as

$$\omega = \frac{2(2n - 1)(z + 1)H' - 3nH}{3nH}. \quad (19)$$

Here, we have two independent equations (17) and (18) with three unknown parameters, called scale factors $a(t)$, ρ and p . To acquire a specified solution, we need an additional equation to solve equation (19). We utilize Gong-Zhang parameter [35] to solve equation (19). Thereafter, now the number of unknowns and equations are in the same number.

$$\omega(z) = \frac{w_0}{z + 1}, \quad (20)$$

where, using the observations the model parameter w_0 may be constrained. In the outline of cosmological modelling, the Gong-Zhang EoS of dark energy (DE) parametrization offers several important advantages. First of all, it offers a framework that can be physically understood with model parameter w_0 denoting the DE EoS parameter at the current epoch ($z = 0$). Also, by clearly including the red-shift dependency in parameterization, we might be able to characterize in what way the DE develops. As the z strategy goes more rapidly towards infinity (in the past), $\omega_{DE}(z) \sim 0$, which demonstrates that the DE EoS parameter leans towards zero at early times. As $z \rightarrow -1$ (in the asymptotic limit), $\omega_{DE}(z) \rightarrow -\infty$, indicates that the DE EoS parameter leans towards negative infinity in the far future. These properties of the DE EoS parameter are reasonable and attractive alternative to study its evolution in $f(R, L_m)$ gravity.

From equation (19) and equation (20), we get

$$\frac{w_0}{z + 1} = \frac{2(2n - 1)(z + 1)H' - 3nH}{3nH}. \quad (21)$$

By solving equation (21), we obtain the Hubble parameter's expression as follows

$$H(z) = h_0 \exp \left(\frac{3n \cdot (zw_o + (z+1) \cdot \log(z+1))}{2(2n-1)(z+1)} \right). \quad (22)$$

where h_0 denotes the current value of the Hubble parameter.

5 Observational constraints

Here, We go ahead with conducting a Bayesian analysis of the current cosmological model for the compatibility of observations. We employ two observational datasets, such as the cosmic chronometer(CC) sample and the joint data sample known as the CC+Pantheon sample, to determine the constraint values h_0 , w_0 and n for the model parameter. We employ the χ^2 minimization methodology with the Markov Chain Monte Carlo(MCMC) technique which is implemented in the emcee Python library [36].

5.1 The observation of Cosmic chronometer dataset

In this section of our research, we observe the observational consequences of our cosmological model. We analyse a data set containing 31 CC data values which continued acquired via the differential ages (DA) process of galaxies in the interior of the range of redshift is $0.07 \leq z \leq 1.965$. This investigation focuses on determining the median values of the model parameters. According to the basic principle set up by Jimenez and Loeb[37], the relationship between the Hubble parameter ($H(z)$), cosmic-time (t), and redshift (z) is stated as follows: $H(z) = \frac{-1}{(1+z)} \frac{dz}{dt}$. By spreading on basic observational constraints, we can determine the model parameters h_0 , w_0 and n through the minimization of the χ^2 function(which is comparable to the maximizing likelihood function) expressed as[38–40].

$$\chi_{CC}^2(\theta) = \sum_{i=1}^{i=31} \frac{[H_{th}(\theta, z_i) - H_{obs}(z_i)]^2}{\sigma_{H(z_i)}^2}. \quad (23)$$

Here, H_{th} characterizes the theoretical value of Hubble, H_{obs} characterizes the observed value, and σ_H characterizes the standard error of the observed value.

The error between the CC data points and the best-fit Hubble parameter curve for the Hubble parameters in equations (22) is displayed in figure (1). Furthermore, Figure (2) represents a contour map demonstrating the 1σ and 2σ likelihood confidence levels for the median values of h_0 , w_0 and n obtained from the CC data.

5.2 The observation of Pantheon dataset

Recently data sample values from the Pantheon supernovae type Ia have been published. They cover 1048 data points and contain 4010 observations for the red-shift range $0.01 < z < 2.26$ is grouped in Ref. [41] and are PanSTARSS1 medium size and PanSTARSS1 light are the two panSTARSS1 [41] in this kit. The research contributes heavily to this work SDSS SNLS Deep Survey, numerous low redshift surveys and HST surveys. The study is also in accordance with CfA1-CfA4 [42, 43] research studies, SDSS [44], SNLS [45], Carnegie Supernova Project (CSP) [46] reinforce the SNIa trial.

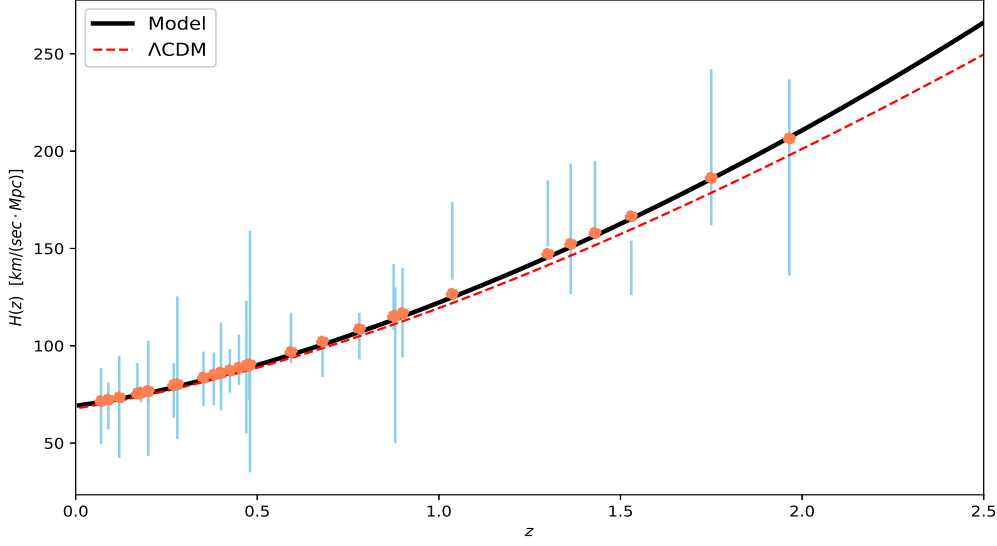


Figure 1: In comparison to the Λ CDM model, the best fit Hubble parameter (given by Eq. (22)) versus z .

The theoretically expected apparent magnitude $\mu_{th}(z)$ is determined by

$$\mu_{th}(z) = M + 5 \log_{10} \left[\frac{d_L(z)}{Mpc} \right] + 25, \quad (24)$$

where M is the absolute magnitude. Also, the luminosity distance $d_L(z)$ may be written as [47]

$$d_L(z) = c(1+z) \int_0^z \frac{dz'}{H(z')}, \quad (25)$$

where the parameter z signifies SNIa's redshift as determined in the cosmic microwave background (CMB) rest frame and c is defined as the light's speed.

The Hubble-free luminosity distance ($D_L(z) \equiv H_0 d_L(z)/c$) is often used in place of the luminosity distance (d_L). We can notice that the Hubble-free luminosity distance is dimensionless whereas the luminosity distance has a dimension called Length. After rewrite the equation (24) represent as,

$$\mu_{th}(z) = M + 5 \log_{10} [D_L(z)] + 5 \log_{10} \left[\frac{c/H_0}{Mpc} \right] + 25. \quad (26)$$

The Parameters M and H_0 may also be utilized to generate a new parameter such as \mathcal{M} , which might be defined as

$$\mathcal{M} \equiv M + 5 \log_{10} \left[\frac{c/H_0}{Mpc} \right] + 25 = M - 5 \log_{10}(h) + 42.38, \quad (27)$$

where $H_0 = h \times 100 \frac{Km}{s.(Mpc)}$. For MCMC analysis, We employ these parameter with appropriate χ^2 for the Pantheon dataset as [48]

$$\chi_P^2 = \nabla \mu_i C_{ij}^{-1} \nabla \mu_j, \quad (28)$$

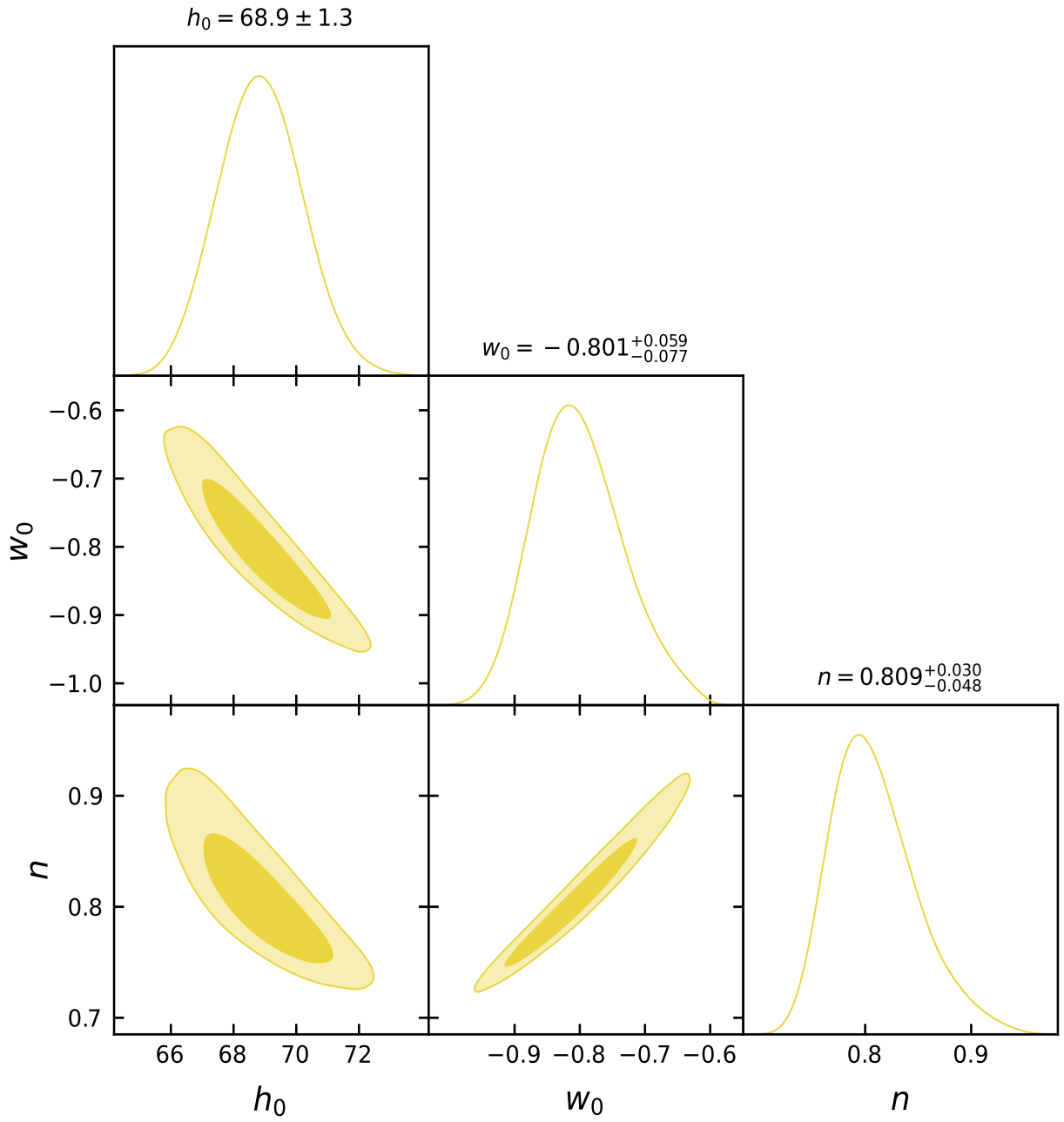


Figure 2: Marginalized 1σ and 2σ contours map with median values of h_0 , w_0 and n for CC data set.

whereas $\nabla\mu_i = \mu_{obs}(z_i) - \mu_{th}(z_i)$, C_{ij}^{-1} defined as the inverse of covariance matrix and μ_{th} may be specified by equation (26).

The luminosity distance is contingent on the Hubble parameter. Previously, we took the emcee package [36] and equation (22) to obtain the maximum likelihood estimate(MLE) by using the combined of CC+Pantheon data-set. The combined χ^2 for MLE is precise as $\chi_{CC}^2 + \chi_P^2$. Figure (3) is exhibited for 1σ and 2σ likelihood contour maps and 1D posterior distributions with MCMC analysis through combined of CC+Pantheon dataset. The median values of model parameters are summarize in Table(1).

Dataset	h_0 [Km/(s.Mpc)]	w_0	n	\mathcal{M}
CC	$68.9^{+1.3}_{-1.3}$	$-0.801^{+0.059}_{-0.077}$	$0.809^{+0.030}_{-0.048}$	-
CC+Pantheon	$69.1^{+1.8}_{-1.8}$	$-0.78^{+0.058}_{-0.066}$	$0.842^{+0.052}_{-0.085}$	$23.807^{+0.013}_{-0.013}$

Table 1: Model parameters' median values in MCMC analysis

6 Result analysis and discussion of Physical, dynamical characteristics of the model

6.1 Analysis of Deceleration parameter

A key factor for the universe's expansion is the deceleration parameter (q). It is a representation of the behaviour of the cosmos. Variations values of the deceleration parameter (q) are used to illustrate the expansion of the universe, the values of the deceleration parameter defined as an accelerated phase for $q < 0$, and the decelerated phase for $q > 0$. When the deceleration parameter is smaller than -1 , the cosmos enters a period of super accelerated expansion. The de Sitter, matter-dominated and radiation-dominated phases of the universe are represented by the values of q i.e. -1 , $\frac{1}{2}$ and 1 , respectively. Deceleration parameter expressed as

$$q = -1 + \frac{d}{dt} \frac{1}{H}. \quad (29)$$

Putting (22) into (29), we get,

$$q(z) = \frac{3nw_0 - (n-2)(z+1)}{2(2n-1)(z+1)}. \quad (30)$$

The analysis of deceleration parameters for the CC and joint data sets is presented in figure (4). Figure (4) demonstrates the transition of the universe's evolution from a decelerated expansion phase to an accelerated expansion phase. This transition occurs at $z = 0.635$ and $z = 0.71$ with median values for CC data and joint data set respectively. The current values of deceleration parameter are $q_0 = -0.6$ (for CC data) and $q_0 = -0.59$ (for joint data).

6.2 Observations of Pressure and Energy Density

The energy density is still positive for the framework of cosmic expansion, although the pressure might become to negative. For the expansion of acceleration of the universe, energy density has been consistently positive while pressure demonstrates negative behavior in the present time and future.

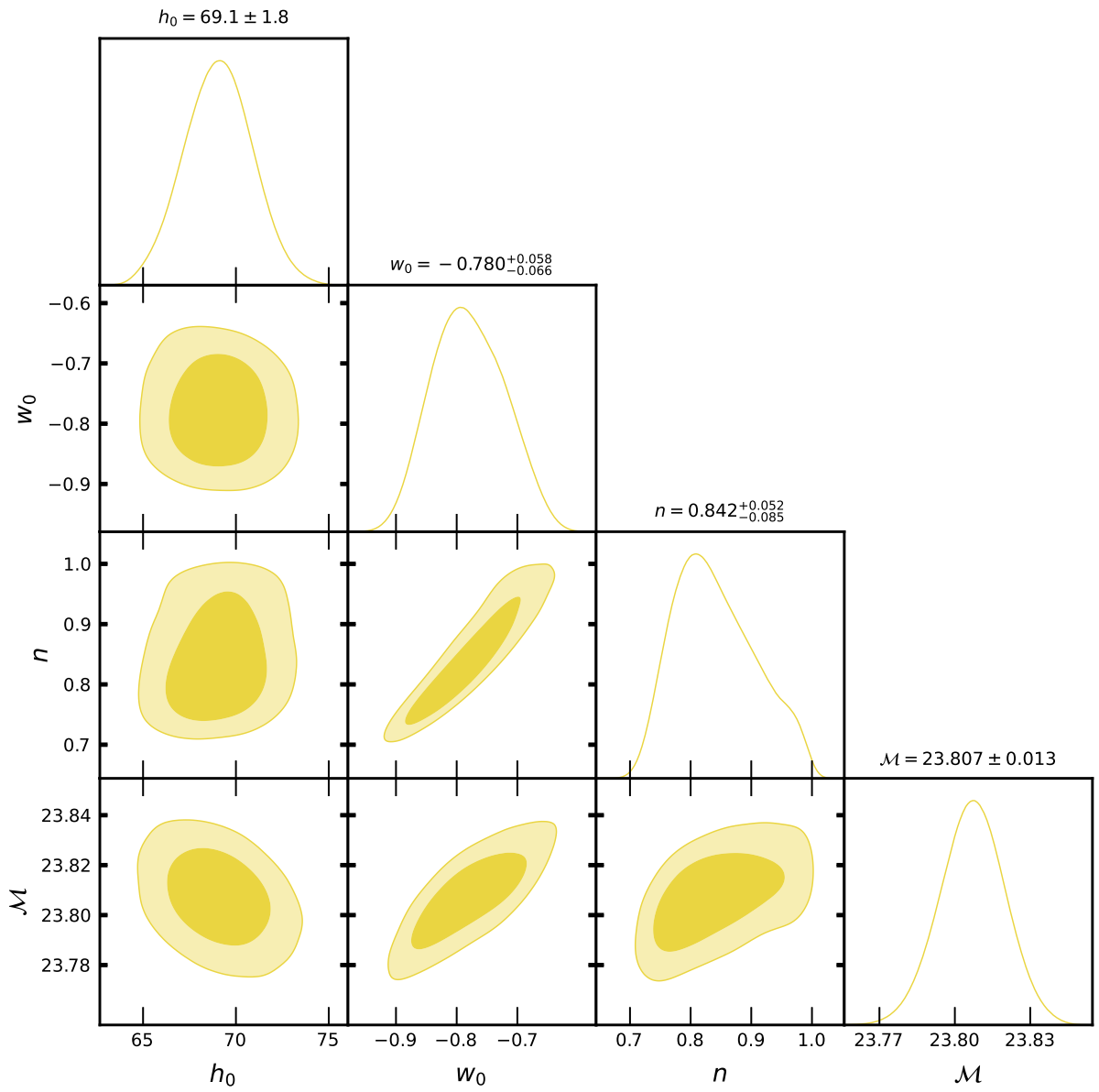


Figure 3: 1σ and 2σ likelihood contours map for h_0 , w_0 , and n for Joint dataset.

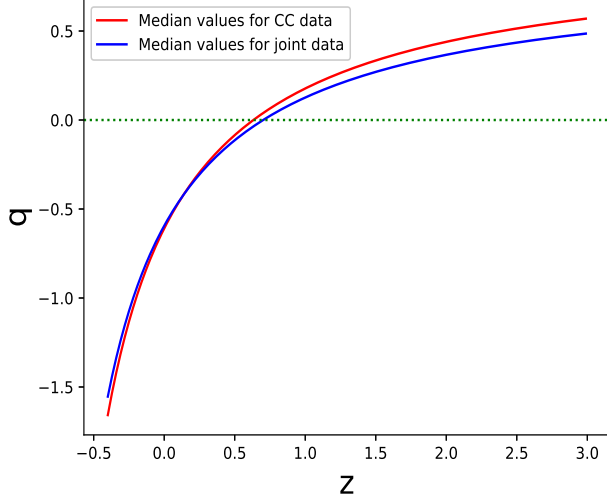


Figure 4: The deceleration parameter(q) versus z .

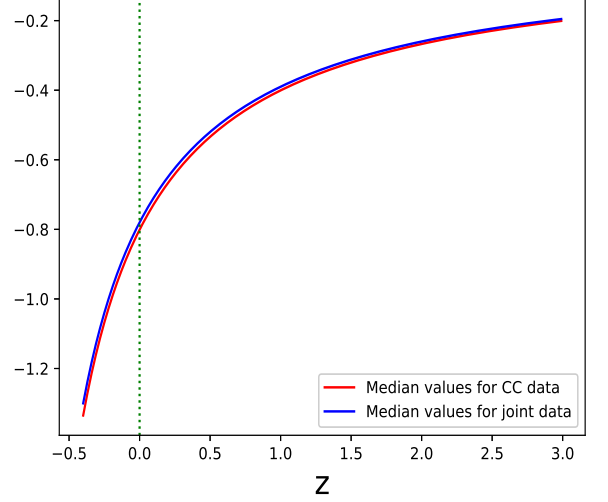


Figure 5: Equation of State parameter (given in Eq. (33)) versus z .

From Using the equations (17) and (22), energy density can be written as :

$$\rho(z) = 3^{1/n} \left(\frac{H_0^2 e^{\frac{3n(\log(z+1) + \frac{z \cdot w_0}{z+1})}{2n-1}}}{2n-1} \right)^{1/n}. \quad (31)$$

From equations (18), (22), and (31), the cosmic pressure can be written as:

$$p(z) = \left[\frac{w_0}{z+1} \right] 3^{1/n} \left(\frac{H_0^2 e^{\frac{3n(\log(z+1) + \frac{z \cdot w_0}{z+1})}{2n-1}}}{2n-1} \right)^{1/n}. \quad (32)$$

The progress of the energy density as well as the pressure is shown in figures (6) and (7) respectively. Significantly, energy density shows a predictable positive behaviour while the pressure shows negative behaviour for the existing and future. These studies are consistent with the accelerating Universe's expanding behaviour.

6.3 Equation of State Parameter

Pressure (p) and energy density (ρ) depends on each other in the universe are shown by the EoS parameter. The dust phase ($\omega = 0$), the radiation-dominated phase ($\omega = \frac{1}{3}$), and the vacuum energy phase ($\omega = -1$) corresponding with the Λ CDM model are some of the some phases seen through the EoS parameter. Furthermore, there is the Universe's accelerating period, which is denoted by ($\omega < -\frac{1}{3}$). The Gong-Zhang EoS parameter ($\omega = \frac{p}{\rho}$) characterised as[35].

$$\omega = \frac{w_0}{z+1}. \quad (33)$$

Here, we are studying the Gong-Zhang EoS parameter, which can be define in equation (33). At present ($z = 0$) the value of this EOS parameter are $\omega = -0.801^{+0.059}_{-0.077}$ (for median values of parameters from CC dataset) and $\omega = -0.78^{+0.058}_{-0.066}$ (for median values of parameters from the joint dataset), respectively. By confining the values of the w_0 parameter from the CC dataset and the combined dataset, Figure (5) illustrates that the EoS parameter represents quintessence behaviour at present for CC and Joint data sets.

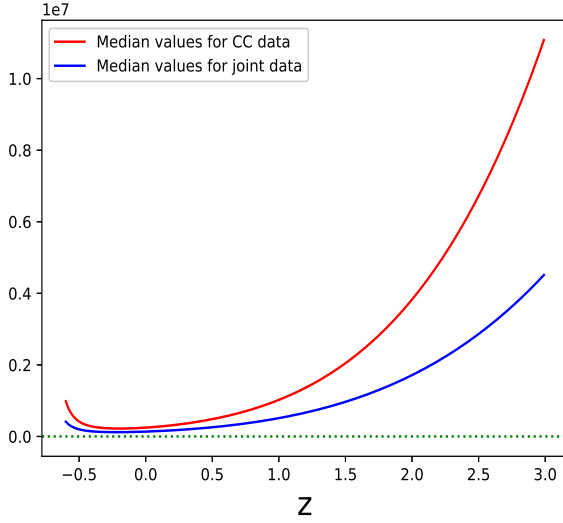


Figure 6: Energy density(ρ) versus z .

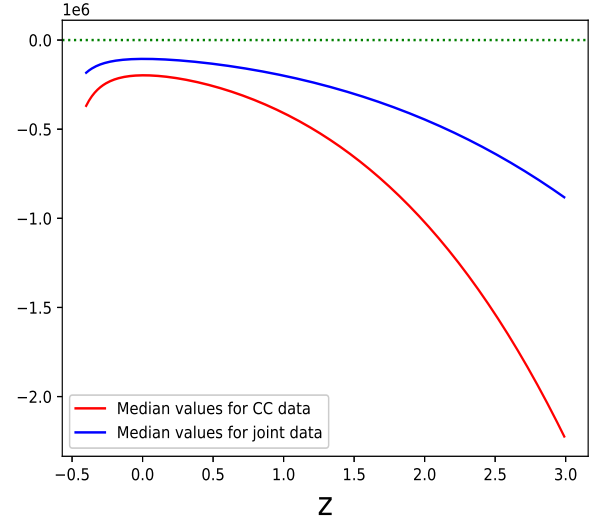


Figure 7: Pressure(p) versus z

6.4 Energy conditions

At a specific point in space-time, the point-wise energy conditions that rely solely on the stress energy tensor are as follows [49–51]:

- NEC:- Null Energy Condition ($\rho + p \geq 0$) always demonstrates that the addition of energy density and pressure is positive. This condition is referred to as the null energy condition.
- WEC:- The condition of weak energy indicates that both of the energy density and the sum of pressure-energy density are non-negative. ($\rho \geq 0$, $\rho + p \geq 0$)
- DEC:- Dominant energy condition statement, i.e. energy density(ρ) remains non-negative and another condition ($\rho \geq |p|$).
- SEC:- Strong energy condition Indicates that the conditions ($\rho + 3p$) remains positive and ($\rho + p$) necessity always be non-negative.

In the scenario of the deceleration stage, the gravitational mass ($\rho + 3p$) continues to be positive. Nevertheless, observational evidence proposes a potential violation of this condition sometime between the era of galaxy formation and the present time. This variation shows the possible presence of negative galactic pressure, that displays anti-gravitational properties. Meanwhile, the Strong Energy Condition (SEC) contains two inequalities, it is important to remember that a violation of one of them would effect a violation of the SEC [49, 52, 53]. Figures (8), (9) and (10) demonstrate the graphical illustration of energy conditions used for this model $f(R, L_m) = \frac{R}{2} + L_m^n$. Moreover, the trajectory of ($\rho + 3p$) turns into positive to negative values at nearly $z = 1.403$ (for CC dataset) and $z = 1.34$ (for the joint dataset). Based on this observations, it can be inferred that this model satisfy all energy conditions (DEC, WEC, SEC and NEC).

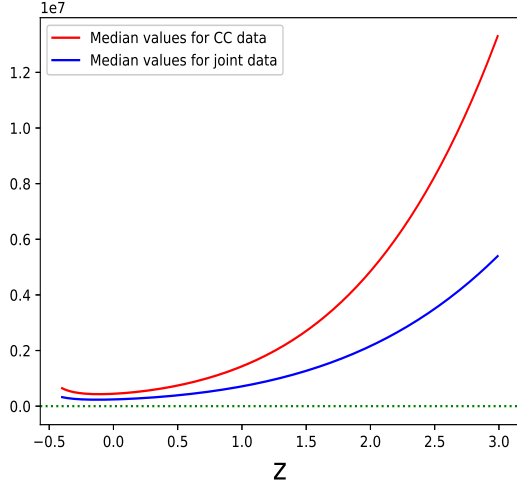


Figure 8: Characteristics of $(\rho - p)$ with z

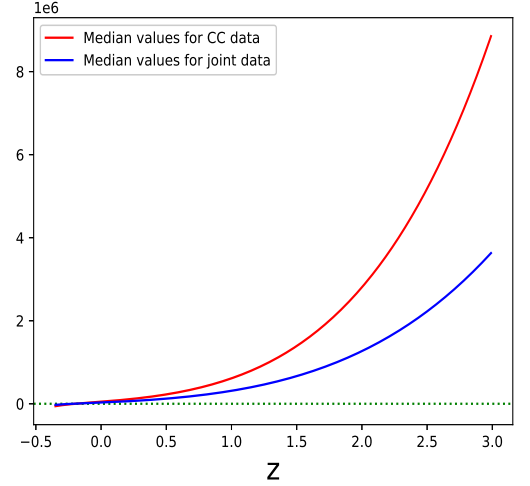


Figure 9: characteristics of $(\rho + p)$ with z

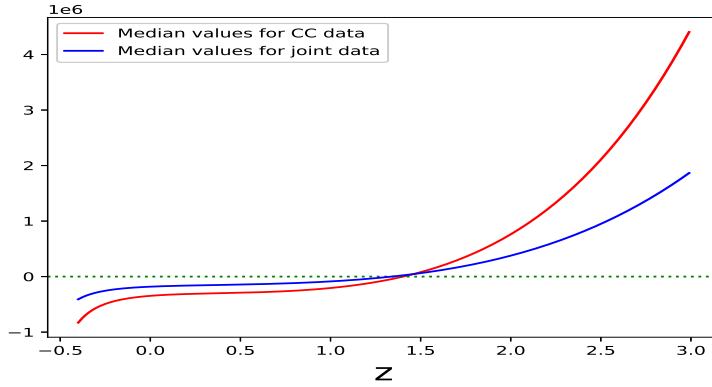


Figure 10: characteristics of $(\rho + 3p)$ with z

6.5 Statefinder diagnostic

It is broadly acknowledged that the geometric physical characteristics of the cosmological model can offer profound intuitions into its dynamical behaviour. To explore different dark energy models other than to the standard Λ CDM model, it becomes vital to analyse additional parameters outside the Hubble parameter H and deceleration parameter q . Higher-order derivatives of the scale factor $a(t)$, other than H and q , occur as indispensable tools to define the dynamical characteristics of the universe. In this matter, Sahni et al. [54, 55] presented a pair of geometrical parameters, symbolised by (r, s) , identified as the *statefinder diagnostics*. These parameters serve as a strong framework to discriminate the evolutionary paths of several dark energy models. The expressions of state finder pair is statistically defined as:

$$r = \frac{\ddot{a}}{aH^3}, \quad s = \frac{r-1}{3(q-\frac{1}{2})}, \quad \text{where } q \neq \frac{1}{2}. \quad (34)$$

These statefinder diagnostic couple (r, s) are described as:

- The Chaplygin gas model is categorized by $r > 1$ and $s < 0$.

- The Λ CDM model obliges as a static point at $(r,s) = (1,0)$.
- Quintessence models are characteristically found in the region $r < 1$ and $s > 0$.
- Holographic dark energy models attribute a static point at $(r,s) = (1, \frac{2}{3})$.
- The standard cold dark matter (SCDM) model links to $(r,s) = (1,1)$.

Figures (11) illustrated the (r,s) trends for the model parameters's median values. In Figure (11), we see that using cosmic chronometer (CC) data set, the trajectory begins in the Chaplygin gas area during initial times, traverses the Λ CDM static point, and ultimately develops into a combined description of dark matter and dark energy.

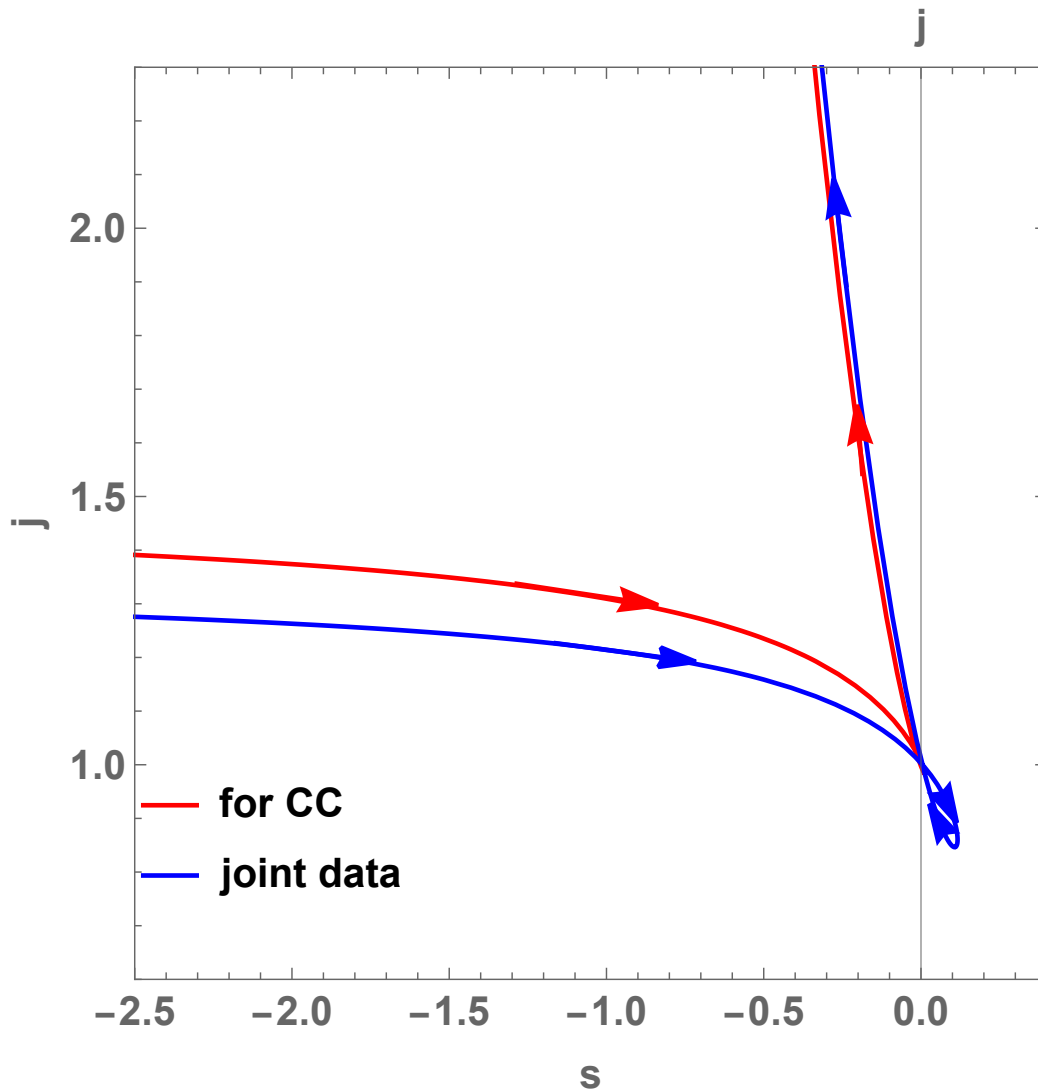


Figure 11: Statefinder (r,s) trajectory

6.6 Age of the Universe

The cosmic age $t(z)$ of a cosmological model can be demonstrated in terms of the redshift z as described in [56]:

$$t(z) = \int_z^\infty \frac{dz}{(1+z)H(z)}. \quad (35)$$

By using the Hubble parameter $H(z)$ existing in equation (22) at present (i.e., $z = 0$), we can calculate the value of this integral and thus calculate the present age of the universe. The age of the universe for this model is $t_0 = 13.22^{+0.165}_{-0.340}$ Gyr (for the CC dataset) and $t_0 = 13.41^{+0.14}_{-0.46}$ Gyr (for the joint data set).

7 Conclusions

This research studies the universe's behaviour for the flat FLRW metric in $f(R, L_m)$ gravity. Then, the equations of motion intended for the flat FLRW space-time metric are calculated. Moreover, the behaviours of the deceleration parameters have been inspected. The deceleration parameter's evolution of the curve demonstrates a recent variation in the universe's phase beginning from decelerated to accelerated. The current values of deceleration parameters are $q_0 = -0.60$ (for CC data) and $q_0 = -0.59$ (for the joint data set) and the value of transition redshift is $z_t = 0.635$ (for the CC data) and $z_t = 0.71$ (for joint data set).

Furthermore, We obtained the median values of model parameters for both data sets. The obtained median values are $h_0 = 68.9^{+1.3}_{-1.3} \text{Km}/(s.mpc)$, $w_0 = -0.801^{+0.059}_{-0.077}$, $n = 0.809^{+0.030}_{-0.048}$ (for CC data) and $h_0 = 69.1^{+1.8}_{-1.8} \text{Km}/(s.mpc)$, $w_0 = -0.78^{+0.058}_{-0.066}$, $n = 0.842^{+0.052}_{-0.085}$ (for joint data set).

The energy density of this model demonstrates positive behaviour while, the pressure has become negative from recent past. Our overall remark is that the model is well-matched with the present-day accelerating universe explanations. The energy conditions are examined to discuss the physical stability of the considered model. Positive behavior is displayed by all energy conditions except SEC, while SEC is violated. The acceleration behavior of cosmic expansion and shift from a decelerated to an accelerated epoch are both strongly supported by the violation of SEC. However, the model is compatible with the present day accelerating universe observations. Lastly, we obtained that the present universe's age is $t_0 = 13.22^{+0.165}_{-0.340}$ Gyr (for the CC dataset) and $t_0 = 13.41^{+0.14}_{-0.46}$ Gyr (for the joint data set).

Acknowledgements

R. Garg thanks to Dr. Ashutosh Singh for the insightful discussions.

References

- [1] A. G. Riess, et al., Observational Evidence from Supernovae for an Accelerating Universe and a Cosmological Constant, *Astronomical Journal* 116 (3) (1998) 1009–1038. doi:<https://doi.org/10.1086/300499>.
- [2] S. Perlmutter, et al., Measurements of Ω and Λ from 42 High-Redshift Supernovae, *Astrophysical Journal* 517 (2) (1999) 565–586. doi:<https://doi.org/10.1086/307221>.
- [3] N. Aghanim, et al., Planck 2018 results. VI. Cosmological parameters, *Astronomy and Astrophysics* 641 (2020) A6. doi:<https://doi.org/10.1051/0004-6361/201833910>.

- [4] S. Weinberg, The cosmological constant problem, *Reviews of modern physics* 61 (1) (1989) 1. doi: <https://doi.org/10.1103/RevModPhys.61.1>.
- [5] S. Ray, U. Mukhopadhyay, X.-H. Meng, Accelerating universe with a dynamic cosmological term, *Gravit. Cosmol.* 13, 142 13 (2007) 142. doi: <https://doi.org/10.48550/arXiv.astro-ph/0407295>.
- [6] R. Kerner, Cosmology without singularity and nonlinear gravitational Lagrangians., *General Relativity and Gravitation* 14 (5) (1982) 453–469. doi: <https://doi.org/10.1007/BF00756329>.
- [7] H. A. Buchdahl, Non-linear lagrangians and cosmological theory, *Monthly Notices of the Royal Astronomical Society* 150 (1) (1970) 1–8. doi: <https://doi.org/10.1093/mnras/150.1.1>.
- [8] T. Harko, F. S. Lobo, S. Nojiri, S. D. Odintsov, $f(r, t)$ gravity, *Physical Review D—Particles, Fields, Gravitation, and Cosmology* 84 (2) (2011) 024020. doi: <https://doi.org/10.1103/PhysRevD.84.024020>.
- [9] Y.-F. Cai, S. Capozziello, M. De Laurentis, E. N. Saridakis, $f(t)$ teleparallel gravity and cosmology, *Reports on Progress in Physics* 79 (10) (2016) 106901. doi: <https://doi.org/10.1088/0034-4885/79/10/106901>.
- [10] S. Capozziello, V. Cardone, H. Farajollahi, A. Ravanpak, Cosmography in $f(t)$ gravity, *Physical Review D—Particles, Fields, Gravitation, and Cosmology* 84 (4) (2011) 043527. doi: <https://doi.org/10.1103/PhysRevD.84.043527>.
- [11] G. P. Singh, R. Garg, A. Singh, A generalized lambda cdm model with parameterized hubble parameter in particle creation, viscous and $f(r)$ model framework, arXiv preprint arXiv:2405.15626 (2024).
- [12] R. Garg, G. P. Singh, A. Singh, Observational constraints on gong-zhang parametrizations in $f(q)$ gravity, arXiv preprint arXiv:2410.18568 (2024).
- [13] G. K. Goswami, R. Rani, J. K. Singh, A. Pradhan, Flrw cosmology in weyl type $f(q)$ gravity and observational constraints, *Journal of High Energy Astrophysics* 43 (2024) 105–113. doi: <https://doi.org/10.1016/j.jheap.2024.06.011>.
- [14] N. Hulke, G. P. Singh, B. K. Bishi, A. Singh, Variable chaplygin gas cosmologies in $f(r, t)$ gravity with particle creation, *New Astronomy* 77 (2020) 101357. doi: <https://doi.org/10.1016/j.newast.2020.101357>.
- [15] G. P. Singh, B. K. Bishi, Bianchi type-i transit universe in $f(r, t)$ $f(r, t)$ modified gravity with quadratic equation of state and λ \varlambda, *Astrophysics and Space Science* 360 (2015) 1–8. doi: <https://doi.org/10.1007/s10509-015-2495-0>.
- [16] A. Singh, Dynamical systems of modified gauss-bonnet gravity cosmological implications, arXiv preprint arXiv:2405.07546 (2024).
- [17] T. Harko, F. S. N. Lobo, $f(r, l_m)$ gravity, *The European Physical Journal C* 70 (2010) 373–379. doi: <https://doi.org/10.1140/epjc/s10052-010-1467-3>.
- [18] V. Faraoni, *Cosmology in scalar tensor gravity* (2004). doi: <https://doi.org/10.1007/978-1-4020-1989-0>.
- [19] P. Zhang, Behavior of $f(r)$ gravity in the solar system, galaxies, and clusters, *Physical Review D* 76 (2) (2007) 024007. doi: <https://doi.org/10.1103/PhysRevD.76.024007>.

- [20] O. Bertolami, J. Páramos, S. G. Turyshev, General theory of relativity: Will it survive the next decade?, in: Lasers, Clocks and Drag-Free Control: Exploration of Relativistic Gravity in Space, Springer, 2008, pp. 27–74. doi:<https://doi.org/10.48550/arXiv.gr-qc/0602016>.
- [21] F. Rahaman, S. Ray, M. Kalam, M. Sarker, Do solar system tests permit higher dimensional general relativity?, Int. J. Theor. Phys. 48 (3) (2009) 3124–3138. doi:<https://doi.org/10.1007/s10773-009-0110-2>.
- [22] S. Nojiri, S. D. Odintsov, Gravity assisted dark energy dominance and cosmic acceleration, Physics Letters B 599 (3-4) (2004) 137–142. doi:<https://doi.org/10.1016/j.physletb.2004.08.045>.
- [23] G. Allemandi et al., Dark energy dominance and cosmic acceleration in first-order formalism, Physical Review D 72 (6) (2005) 063505. doi:<https://doi.org/10.1103/PhysRevD.72.063505>.
- [24] G. Manna et al., $f(r, l_x)$ -gravity in the context of dark energy with power law expansion and energy conditions, Chinese Physics C 47 (2) (2023) 025101. doi:<https://doi.org/10.1088/1674-1137/ac9fbe>.
- [25] F. S. N. Lobo, T. Harko, Extended $f(R, L_m)$ theories of gravity, 2015.
- [26] R. Garg, G. P. Singh, A. R. Lalke, S. Ray, Cosmological model with linear equation of state parameter in $f(r, l_m)$ gravity, Physics Letters A 525 (2024) 129937. doi:<https://doi.org/10.1016/j.physleta.2024.129937>.
- [27] A. Pradhan, D. C. Maurya, G. K. Goswami, A. Beesham, Modeling transit dark energy in $f(r, l_m)$ -gravity, International Journal of Geometric Methods in Modern Physics 20 (06) (2023) 2350105. doi:<https://doi.org/10.1142/S0219887823501050>.
- [28] B. K. Shukla, R. K. Tiwari, D. Sofuoğlu, A. Beesham, Flrw universe in $f(r, l_m)$ gravity with equation of state parameter, East European Journal of Physics (4) (2023) 376–389. doi:<https://doi.org/10.26565/2312-4334-2023-4-48>.
- [29] D. C. Maurya, Bianchi-i dark energy cosmological model in $f(r, l_m)$ -gravity., International Journal of Geometric Methods in Modern Physics 21 (4) (2024). doi:<https://doi.org/10.1142/S0219887824500725>.
- [30] A. Shukla, R. Raushan, R. Chaubey, Dynamical systems analysis of $f(r, l_m)$ gravity model, arXiv preprint arXiv:2308.06519 (2023).
- [31] L. V. Jaybhaye, et al., Cosmology in $f(r, l_m)$ gravity, Physics Letters B 831 (2022) 137148. doi:<https://doi.org/10.1016/j.physletb.2022.137148>.
- [32] B. Ryden, Introduction to cosmology addison wesley san francisco (2003).
- [33] T. Harko, F. S. N. Lobo, Generalized curvature-matter couplings in modified gravity, Galaxies 2 (3) (2014) 410–465. doi:<https://doi.org/10.3390/galaxies2030410>.
- [34] T. Harko et. al., Gravitational induced particle production through a nonminimal curvature–matter coupling, The European Physical Journal C 75 (2015) 1–15. doi:<https://doi.org/10.1140/epjc/s10052-015-3620-5>.
- [35] Y. Gong, Y.-Z. Zhang, Probing the curvature and dark energy, Physical Review D 72 (4) (2005) 043518. doi:<https://doi.org/10.1103/PhysRevD.72.043518>.

- [36] D. Foreman-Mackey et al., emcee: the mcmc hammer, *Publications of the Astronomical Society of the Pacific* 125 (925) (2013) 306. doi:[10.1086/670067](https://doi.org/10.1086/670067).
- [37] R. Jimenez, A. Loeb, Constraining cosmological parameters based on relative galaxy ages, *The Astrophysical Journal* 573 (1) (2002) 37. doi:<https://doi.org/10.1086/340549>.
- [38] S. Mandal, A. Singh, R. Chaubey, Late-time constraints on barotropic fluid cosmology, *Physics Letters A* 519 (2024) 129714. doi:<https://doi.org/10.1016/j.physleta.2024.129714>.
- [39] S. Mandal, A. Singh, R. Chaubey, Cosmic evolution of holographic dark energy in $f(q, t)$ gravity, *International Journal of Geometric Methods in Modern Physics* 20 (05) (2023) 2350084. doi:<https://doi.org/10.1142/S0219887823500846>.
- [40] A. Singh, S. Krishnannair, Affine eos cosmologies: Observational and dynamical system constraints, *Astronomy and Computing* 47 (2024) 100827. doi:<https://doi.org/10.1016/j.ascom.2024.100827>.
- [41] D. M. Scolnic, et al., The complete light-curve sample of spectroscopically confirmed sne ia from pan-starrs1 and cosmological constraints from the combined pantheon sample, *The Astrophysical Journal* 859 (2) (2018) 101. doi:<https://doi.org/10.3847/1538-4357/aab9bb>.
- [42] A. G. Riess, et al., BVRI light curves for 22 type ia supernovae, *The Astronomical Journal* 117 (2) (1999) 707. doi:<https://doi.org/10.1086/300738>.
- [43] M. Hicken, et al., Improved dark energy constraints from 100 new cfa supernova type ia light curves, *The Astrophysical Journal* 700 (2) (2009) 1097. doi:<https://doi.org/10.1088/0004-637X/700/2/1097>.
- [44] M. Sako, et al., The data release of the sloan digital sky survey-ii supernova survey, *Publications of the Astronomical Society of the Pacific* 130 (988) (2018) 064002. doi:[10.1088/1538-3873/aab4e0](https://doi.org/10.1088/1538-3873/aab4e0).
- [45] J. Guy, et al., The supernova legacy survey 3-year sample: Type ia supernovae photometric distances and cosmological constraints, *Astronomy & Astrophysics* 523 (2010) A7. doi:<https://doi.org/10.1051/0004-6361/201014468>.
- [46] C. Contreras, et al., The carnegie supernova project: first photometry data release of low-redshift type ia supernovae, *The Astronomical Journal* 139 (2) (2010) 519. doi:[10.1088/0004-6256/139/2/519](https://doi.org/10.1088/0004-6256/139/2/519).
- [47] S. D. Odintsov, et al., Cosmological fluids with logarithmic equation of state, *Annals of Physics* 398 (2018) 238–253. doi:<https://doi.org/10.1016/j.aop.2018.09.015>.
- [48] K. Asvesta, et al., Observational constraints on the deceleration parameter in a tilted universe, *Monthly Notices of the Royal Astronomical Society* 513 (2) (2022) 2394–2406. doi:<https://doi.org/10.1093/mnras/stac922>.
- [49] A. Singh et al., Lagrangian formulation and implications of barotropic fluid cosmologies, *International Journal of Geometric Methods in Modern Physics* 19 (07) (2022) 2250107. doi:<https://doi.org/10.1142/S0219887822501079>.
- [50] M. Visser, Energy conditions in the epoch of galaxy formation, *Science* 276 (5309) (1997) 88–90. doi:<https://doi.org/10.1126/science.276.5309.88>.

- [51] G. P. Singh, A. R. Lalke, Cosmological study with hyperbolic solution in modified $f(q, t)$ gravity theory, *Indian Journal of Physics* 96 (14) (2022) 4361–4372. doi:<https://doi.org/10.1007/s12648-022-02341-z>.
- [52] A. Singh, Homogeneous and anisotropic cosmologies with affine eos: a dynamical system perspective, *The European Physical Journal C* 83 (8) (2023) 696. doi:<https://doi.org/10.1140/epjc/s10052-023-11879-z>.
- [53] A. R. Lalke, G. P. Singh, A. Singh, Late-time acceleration from ekpyrotic bounce in $f(q, t)$ gravity, *International Journal of Geometric Methods in Modern Physics* 20 (08) (2023) 2350131. doi:<https://doi.org/10.1142/S0219887823501311>.
- [54] V. Sahni, T. D. Saini, A. A. Starobinsky, U. Alam, Statefinder—a new geometrical diagnostic of dark energy, *Journal of Experimental and Theoretical Physics Letters* 77 (2003) 201–206. doi:<https://doi.org/10.1134/1.1574831>.
- [55] U. Alam, V. Sahni, T. Deep Saini, A. Starobinsky, Exploring the expanding universe and dark energy using the statefinder diagnostic, *Monthly Notices of the Royal Astronomical Society* 344 (4) (2003) 1057–1074. doi:<https://doi.org/10.1046/j.1365-8711.2003.06871.x>.
- [56] M.-L. Tong, Y. Zhang, Cosmic age, statefinder, and om diagnostics in the decaying vacuum cosmology, *Physical Review D* 80 (2) (2009) 023503. doi:<https://doi.org/10.1103/PhysRevD.80.023503>.